Scanning Microscopy

Volume 9 | Number 1 Article 19

3-31-1995

The Effects of Diethyldithiocarbamate (DDC) on the Astrocytic Cytoskeleton

Mary F. McManus
St. John's University, Jamaica

Louis D. Trombetta
St. John's University, Jamaica

Scanning Microscopy, Vol. 9, No. 1, 1995 (Pages 257-270) 0891-7035/95$5.00+.25
Scanning Microscopy International, Chicago (AMF O'Hare), IL 60666 USA

THE EFFECTS OF DIETHYLDITHIOCARBAMATE (DDC) ON THE ASTROCYTIC CYTOSKELETON

Mary F. McManus and Louis D. Trombetta*

College of Pharmacy and Allied Health Professions, Toxicology Program
St. John's University, Jamaica, New York

(Received for publication April 18, 1994 and in revised form March 31, 1995)

Abstract

The dithiocarbamates are a group of compounds that are used extensively in industry, agriculture and medicine. Exposure to these compounds has caused deleterious effects to both the central and peripheral nervous systems. Cultured rat hippocampal astroglia treated with 35 μg/ml diethyldithiocarbamate (DDC) in media were studied for alterations to the cytoskeleton. Examination by both immunohistochemistry and scanning electron microscopy revealed disruption of the cytoskeletal elements. This occurred in a progressive time-dependent manner. Electrophoretic patterns demonstrated two cytoskeletal protein alterations. The microtubular protein, β-tubulin, appeared to have an altered mobility while the major intermediate filament protein, glial fibrillary acidic protein (GFAP), was decreased. The cytoskeleton appears to be an important cellular target for injury by DDC exposure. This study has demonstrated that DDC induces alterations in the architecture of the cytoskeleton of astroglia and suggests that these changes involve microtubular and intermediate filament proteins.

Key Words: Astrocyte, carbamates, cytoskeleton, diethyldithiocarbamate, DDC, glial fibrillary acidic protein, intermediate filaments, microtubules, neurotoxicity, tubulin.

*Address for correspondence:
Louis D. Trombetta
College of Pharmacy and Allied Health Professions,
St. John's University,
8000 Utopia Parkway,
Jamaica, NY 11439

Telephone number: (718) 990-6025
FAX number: (718) 969-0753

Introduction

The nervous system is a rich source of cytoskeletal proteins that assume critical roles in determining and maintaining the integrity of nervous tissue structure and function. Many of the neurodegenerative diseases are characterized by alterations to filamentous proteins resulting in compromised cellular function or cell death. Alterations in cytoskeletal architecture have also been associated with aging processes (Goldman and Yen, 1986). The abnormalities of cytoskeletal structure seen in many neurotoxic and neurodegenerative diseases include abnormal cross-linking, oxidation of essential membrane or protein sulfhydryl groups, lipid peroxidative injury and altered calcium homeostasis (Marcum *et al.*, 1978; Lehto *et al.*, 1984; Li *et al.*, 1987; Li and Chou, 1992).

Neurotoxic substances are often associated with the pathogenesis of the cytoskeleton. Profoundly abnormal arrangements and distortions of cytoskeletal elements have been described within neuronal and glial cells (Ghetti, 1979; Griffin *et al.*, 1983). The experimental disruption of cytoskeletal elements contributes to the understanding of the pathogenesis of both toxic and degenerative alterations.

This paper addresses the problem of neurotoxic injury to the cytoskeleton produced by exposure to the dithiocarbamates, specifically diethyldithiocarbamate (DDC). The dithiocarbamates have had extensive applications in industry, agriculture, and medicine (Cohen and Robins, 1990). They are extremely reactive compounds due to their metal-chelating characteristics, interactions with sulfhydryl groups and enhancement of oxidative reactions. These compounds are known inhibitors of many metal-dependent and sulfhydryl enzyme systems (Miller, 1982).

The dithiocarbamates have been shown to induce degenerative changes in both the central and peripheral nervous systems (Adachi and Solitaire, 1979; Anzil, 1985). Observations, in a rat model, by transmission electron microscopy, at the earliest stages of insult, show large numbers of microtubules and neurofilaments in various stages of degeneration (Ansbacher *et al.*,

1982; Trombetta and Adachi, 1985). Early degenerative changes were noted in astroglial cells months prior to neuronal damage, suggesting that the astrocyte may be the initial target for DDC-induced injury (Trombetta and Adachi, 1985).

DDC is a sulfhydryl-containing chelator that is capable of forming a bis-(DDC)-metal complex (Johansson and Stankiewicz, 1985). Because of it's highly lipophilic character, this complex can readily pass through membrane barriers, resulting in an observable increase in intracellular metal concentration (Johansson and Stankiewicz, 1985; Andersen *et al.*, 1988). The cytotoxic action may be mediated by the chelating properties of the compound, resulting in inhibitory effects on a variety of cellular functions (Tempel *et al.*, 1985), or by the formation of disulfide linkages with essential proteins (Stromme, 1963). This affinity offers some clinical application in the treatment of metal toxicity (Weiss *et al.*, 1990) and has also been used to ameliorate the nephrotoxic effects of the antineoplastic agent cisplatin (Borch and Pleasants, 1979). DDC has been used as an antiviral agent because of it's ability to bind zinc-dependent gene products essential for viral replication *in vitro* (Hutchinson, 1985). Recently, it has also been investigated as an immuno-modulatory agent (Hersh *et al.*, 1993).

In vitro studies with DDC by Trombetta *et al.* (1988) have attributed toxicity to the overwhelming influx of copper (greater than a 400% increase) in treated cells. DDC alters copper homeostasis by it's potent chelating ability. The bis-(DDC)-copper complex has been shown to redistribute copper to the central nervous system (Johansson and Stankiewicz, 1985; Allain and Krari, 1991). Copper-induced cytotoxicity may be due to this complex binding to cellular macromolecules resulting in generation of reactive free radical species (Tempel *et al.*, 1985; Allain and Krari, 1991). Cupric ions also react with membrane sulfhydryl groups resulting in the formation of superoxide radicals that are capable of initiating lipid peroxidation (Hochstein *et al.*, 1980). Some of the toxic effects of DDC could be explained by this mechanism.

The astrocyte is an essential modulator of normal central nervous system (CNS) activity. In the adult CNS, it retains a close functional relationship with neurons and plays an important role in neuronal metabolism by maintaining the microenvironment that surrounds each neuron (Koestner and Norton, 1991). A ratio of 10 astrocytes to each neuron is not uncommon in some areas of the brain (Koestner and Norton, 1991).

The astrocyte, like other eukaryotic cells, is dependent upon a highly organized internal structure composed of a complex network of filamentous proteins. These proteins are classified into three widely distributed fiber systems which, in concert, form the cytoskeleton. There is a structural and functional interdependence of these fiber systems, and therefore, any disruption may result in a variety of cellular changes. Alterations in cytoskeletal organization can cause irreparable harm to cellular homeostasis.

The cytoskeleton plays a major role in determination of cell shape, cell motility, cellular division, intracellular transport, and spatial organization of cellular components (Bernal and Stahel, 1985). The principal structures comprising the cytoskeleton are the microtubules, intermediate filaments, microfilaments, and the associated cytoskeletal proteins (Alberts *et al.*, 1989). The major protein of the microtubule system is tubulin. Intermediate filaments in astroglia are characterized by glial fibrillary acidic protein (GFAP) (Hansson *et al.*, 1984) and microfilaments are primarily composed of actin (Alberts *et al.*, 1989).

Conditions, which may alter states of polymerization or the interaction of different cytoskeletal elements, may change cell shape or cause the formation of abnormal filamentous aggregates within cells. The latter may be the case in Alzheimer's disease or other neurodegenerative diseases where neurofibrillary tangles are found. These inclusions cross-react with antibodies directed against neurofilaments, microtubule associated proteins (MAPs), and vimentin. Other cytoskeletal abnormalities include Pick Bodies which cross-react with antibodies directed against neurofilaments and tubulin, Lewy Bodies which cross-react with antibodies directed against neurofilaments, and Hirano Bodies which react with actin antibodies (Goldman and Yen, 1986).

The purpose of this study is to investigate the cytotoxic effects of diethyldithiocarbamate on cultured astroglial cells with respect to cytoskeletal alterations. The astroglial model system has been chosen because of early *in vivo* degenerative changes found in astrocytes during chronic low dose exposure (Trombetta and Adachi, 1985).

Materials and Methods

Cell culture

Establishment of Astrocyte Cultures. The astrocyte cultures were obtained from the hippocampus of Sprague Dawley rat pups, postnatal day one. Cultures were grown in Dulbecco's modified Eagle medium (DMEM) containing 4.5 g glucose, glutamine, and 25 mM HEPES buffer per liter supplemented with 10% fetal bovine serum, 0.1 mg/ml streptomycin, and 100 u/ml penicillin (complete medium). Cultures were incubated at 37°C in an atmosphere containing 92% air and 8% CO_2. The method used yields astrocyte cultures that are more than 95% pure as established by immuno-stain-

ing for glial fibrillary acidic protein (GFAP), an astrocyte-specific marker (Trombetta *et al.*, 1988).

Experimental protocol

For all experiments, an aliquot of the trypsinized resuspended cells was removed and counted in a hemocytometer. The cells were plated at equal densities into appropriate cultureware (flasks, glass slides or onto 12 mm round glass coverslips). Exponentially replicating cells of the same passage number were grown to a subconfluent monolayer prior to DDC exposure. By 48 hours after plating, astrocytes contained a well-organized cytoskeleton and expressed GFAP. DDC exposure began at this time period. In all experiments, the responses of DDC-treated cell populations were compared to control cells from the same passage.

The trihydrate sodium salt of diethyldithiocarbamate (DDC) was prepared in complete medium and filter sterilized just prior to use. The cells were exposed for one hour to 35 μg/ml DDC (1.5×10^{-4} M) (Trombetta *et al.*, 1988). All cells were then rinsed with one wash of Dulbecco's phosphate buffered saline (PBS) and refed with complete medium. Cell suspensions were then plated into flasks or onto coverslips. Control and experimental cultures were harvested at 4, 8, 12, and 24 hours post treatment. These time periods were selected because of specific morphologic and biochemical characteristics (Trombetta *et al.*, 1988; Stein and Trombetta, 1993; Simonian *et al.*, 1992).

Immunohistochemistry

Cells were plated and grown to subconfluency on glass Lab-Tek® chamber slides and treated according to experimental protocol. The cells were rinsed with Dulbecco's PBS at 25°C and then washed for 15 seconds at 25°C with a mixture of 0.1% Triton X-100 and 0.125% glutaraldehyde in Dulbecco's PBS. The cells were then washed with Dulbecco's PBS once and fixed in 0.25% glutaraldehyde for 10 minutes. The chamber slides were incubated with heat-inactivated goat serum in Dulbecco's PBS (1:20) for 30 minutes. The goat serum was shaken off and the chamber slides were flooded with either dilute primary β-tubulin antibody (1:400) or dilute primary glial fibrillary acidic protein antibody (1:800) and incubated for 1 hour. The slides were washed thoroughly in several changes of deionized distilled water to remove unbound antibody. Diluted gold-conjugated secondary antibody was added to the chambers and incubated for 1 hour. Slides were washed thoroughly with deionized distilled water to remove unbound gold particles. The gold labeling was enhanced with silver for visualization. Slides were immersed in 0.2 M sodium citrate buffer for 5 minutes to reduce the pH to 3.5 (this slows down the silver enhancement reaction) and then placed in silver enhancement solution (Zymed, San Francisco, CA). The slides were developed for 12 minutes and immersed in photographic fixative for 5 minutes.

Scanning electron microscopy

Whole cell architecture. Cells were grown to subconfluence on 12 mm round cover slips in complete medium and treated according to experimental protocol. The cells were fixed with 1.5% glutaraldehyde in Dulbecco's PBS for 1 hour at room temperature. Dehydration was achieved by a series of acetone-water steps by gently aspirating off half of the old solution and adding new. Coverslips were critically point dried (CPD) in a Polaron E 3000 drier using bone dry CO_2 as the transition fluid. The specimens were then cold sputter coated with 15 nm of gold using a Polaron E 5100, series II coater for 60 seconds set at 2.5 kV. Specimens were viewed with a eucentric stage on a Hitachi S-530 scanning electron microscope (SEM) operated at an accelerating voltage of 25 kV.

Cytoskeletal architecture. Cells were grown to subconfluence on 12 mm round cover slips in complete medium. The cells were treated as previously described and the cytoskeletons prepared for SEM according to the method of Bell *et al.* (1988).

Scanning electron microscopy is the method of choice to examine the cytoskeleton because the spatial distribution of the component parts are readily apparent (Bell, 1981). At the end of each specified time period, the cells were rinsed twice with calcium-free PBS, pH 7.4, at 37°C to remove contaminants. If the calcium in the growth medium is not removed by rinsing, microtubules may depolymerize and thus be partially or completely lost (Bell, 1981). Additionally, serum proteins in the media must be removed as they may contaminate the extracted cytoskeletons.

Fixation of the cells prior to lysis was carried out with the reversible protein cross-linker dithiobis(succinimidyl propionate) (DSP) from Pierce (Rockford, IL). The cells were cross-linked to the substratum with DSP dissolved in PBS supplied with 1 g/l glucose at 37°C for 10 minutes. A stock solution of 20 mg/ml DSP was prepared in dimethylsulfoxide (Eastman Kodak Co., Rochester, NY). This solution was diluted 1:100 in the appropriate buffer immediately before use. The purpose of prefixing with DSP was to stabilize the cytoskeleton in order to help it withstand the rigors of the extraction procedure (Bell, 1981). Prefixation also markedly improves the quantitative retention of cytoskeletal structures.

Subsequent to initial cross-linking, the cells were extracted with 0.5% Triton X-100 in microtubule stabilizing buffer (MSB) containing DSP and maintained at 37°C for 10 minutes. MSB consists of 1 mM ethylene glycolbis(2-aminoethylether)-N,N,N',N'-tetraaceticacid

(EGTA), 4% polyethylene glycol 6000 (PEG 6000), 100 mM piperazine-N,N'-bis(2-ethane-sulfonicacid) (PIPES) and 0.0015% phenol red (Eastman Kodak, Rochester, NY), pH 6.9. Cells were extracted further with two washes of 0.5% Triton X-100 in MSB for 5 minutes each. They were exposed to a fourth detergent wash containing 2.5% glutaraldehyde (GA) for 30 minutes at 25°C. Cytoskeletons were post-fixed with 2.5% GA in a rinsing buffer (RB) for 12 hours at 4°C. The RB consisted of 0.1 M sucrose and 0.1 M cacodylate buffer, pH 7.2. The cytoskeletons were rinsed three times with RB for 5 minutes each and placed into a distilled water rinse. Dehydration was achieved by a series of acetone-water steps by gently aspirating off half of the old solution and adding new. Subsequently, the cytoskeletons were dehydrated, critical point dried, sputter coated, and viewed as described above.

SDS-PAGE of cytoskeletal extracts

Cells were grown in 75 cm^2 flasks and treated according to the protocol described above. The cells from each experiment were harvested and protein extracted according to the method of Bell *et al.* (1988). This procedure is detailed above in the **SEM** section up to the second extraction/fixation step. The flasks were then gently rinsed twice with MSB at 37°C. The cells were fully extracted with 0.5% Triton X-100 in MSB for 5 minutes with gentle rocking. This last step was followed by two additional washes of MSB. The cells were then scraped down in the final MSB wash to be pooled and centrifuged. The resulting pellet was suspended in 1 or 2 ml of MSB and stored in a cryovial at -70°C for future use. When removed from the freezer, the suspension was micro-homogenized under cold conditions.

Aliquots of samples were removed from the stock and diluted in tracking buffer containing 0.125 M Tris-Cl, pH 6.8, 4% SDS, 20% glycerol, and 10% 2-mercaptoethanol. Samples were run on SDS-polyacrylamide gels. The gels were prepared according to the Laemmli (1970) system with a 10% slab and a 4% stacking gel. These gels were prepared fresh for each run, which was carried out in running buffer at room temperature, consisting of 0.1% SDS-0.025 M Tris-glycine buffer pH 8.8. All electrophoreses were performed in duplicate on the SE 250 Mighty Small II (Hoefer Scientific Instruments, San Francisco, CA). Gels were stained overnight with 0.125% Coomassie Brilliant Blue R in 50% methanol and 10% acetic acid. They were destained for 1 hour in 50% methanol and 10% acetic acid, and then placed in 7% acetic acid and 5% methanol.

Protein concentrations for treated and control samples were all normalized before loading into sample wells. Rainbow markers (Amersham, Arlington Heights, IL) with a range of molecular weights from 200 to 14.3 kD were used. A second set of markers in the high molecular weight range were also used (Sigma, St. Louis, MO). The molecular weights of these markers ranged from 205 to 29 kD.

Figure 1. Phase contrast micrograph of control rat astrocytes in culture. The peripheral regions of the cells (solid arrows) are more translucent than their perinuclear regions (open arrows).

Figure 2. Electron micrograph of a control astrocyte. Note that in the peripheral region rod-like structures can be seen under the plasmalemma. These structures may represent the underlying cytoskeleton. Sometimes in the perinuclear region of the cell a punctate cell surface could be seen. These openings did not appear artifactual since they showed a continuous cell membrane. Nucleus (N); Perinuclear region (NR); Peripheral region (PR).

Figure 3. Light micrograph of a control astrocyte immunohistochemically stained with colloidal gold for β-tubulin. Notice the ray-like projection from the juxtanuclear region. This region probably represents the region of the centrosome.

Figure 4. Light micrograph of a control astrocyte immunohistochemically stained for β-tubulin. Note that the microtubules radiate from the center of the cell; turn and run parallel to the cell perimeter.

Figure 5. Light micrograph of a control astrocyte immunohistochemically stained for GFAP. Note that the fibers lack polarity and appear more randomly distributed than those composed of tubulin.

Figure 6. Light micrograph of a control astrocyte immunohistochemically stained for GFAP. Notice the fine interlacing network of fibers extending into the periphery of the cell.

Western blot analysis

Upon completion of the PAGE electrophoresis, one gel was immediately placed in the Coomassie blue stain while the other was transferred to a 0.45 μm nitrocellulose using a TE 22 Mighty Small™ Transphor unit (Hoefer Scientific Instruments). The alkaline phosphatase immunoblot kit from Zymed (San Francisco, CA) containing a biotinylated anti-mouse IgG conjugate was used for the detection of antigen-antibody binding. The three primary antibodies that were used for protein analysis were anti-β-tubulin, anti-GFAP, and anti-actin. All primary antibodies were diluted in PBS containing 1% BSA. Monoclonal anti-β-tubulin (Sigma) was used at the recommended dilution of 1:400, monoclonal glial fibrillary acidic protein (Sigma) was diluted 1:200 and monoclonal anti-actin (Sigma) was diluted 1:600. All blots were incubated with chromagen and preserved with a 10% solution of glycerol in water.

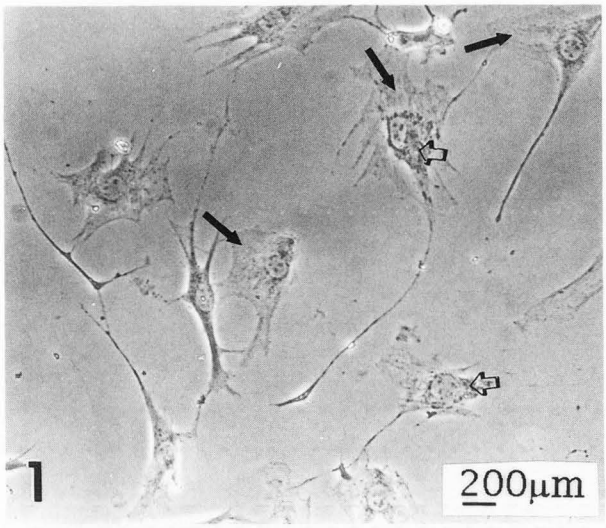
1
200μm

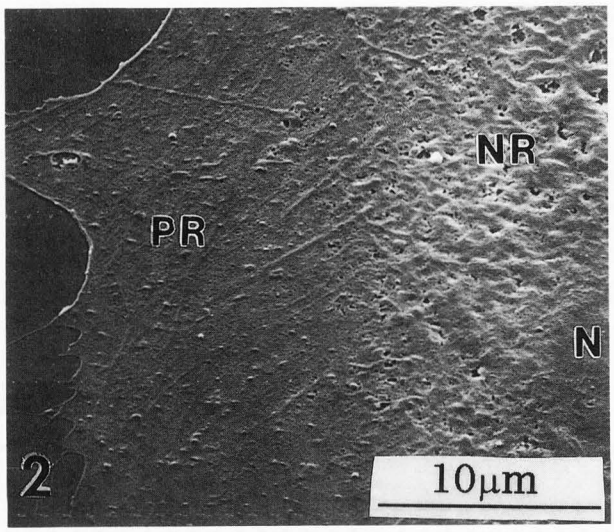
NR
PR
N
2
10μm

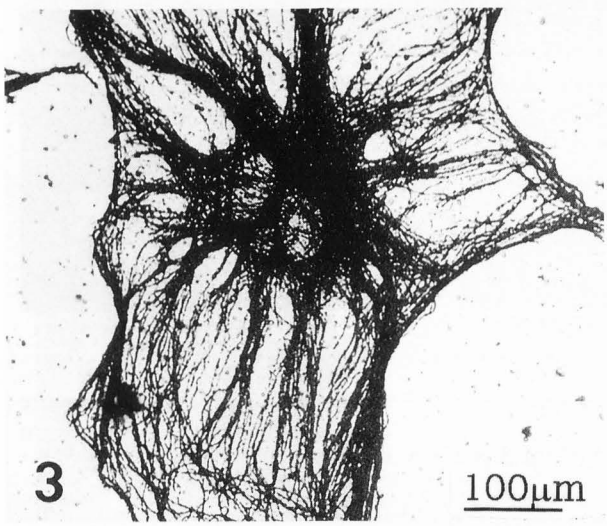
3
100μm

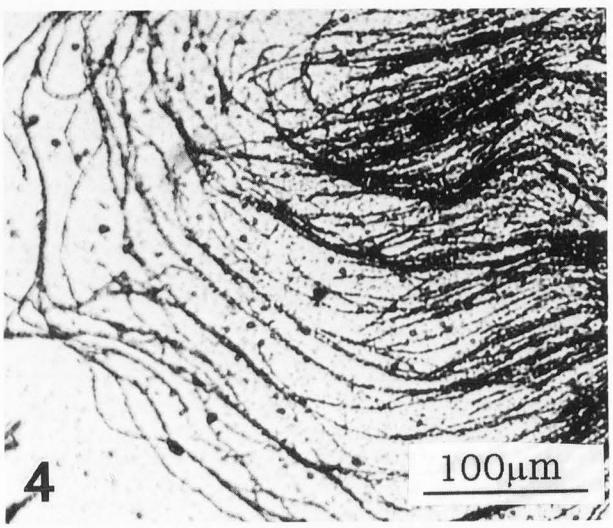
4
100μm

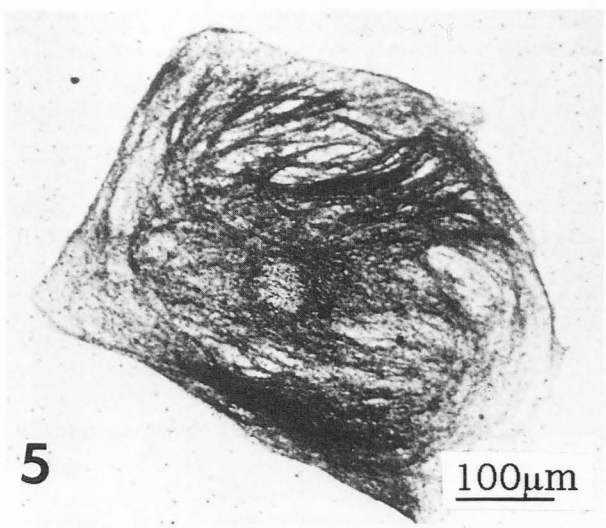
5
100μm

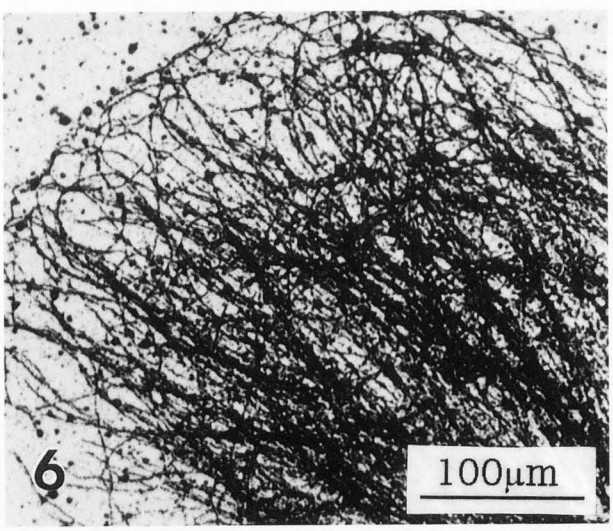
6
100μm

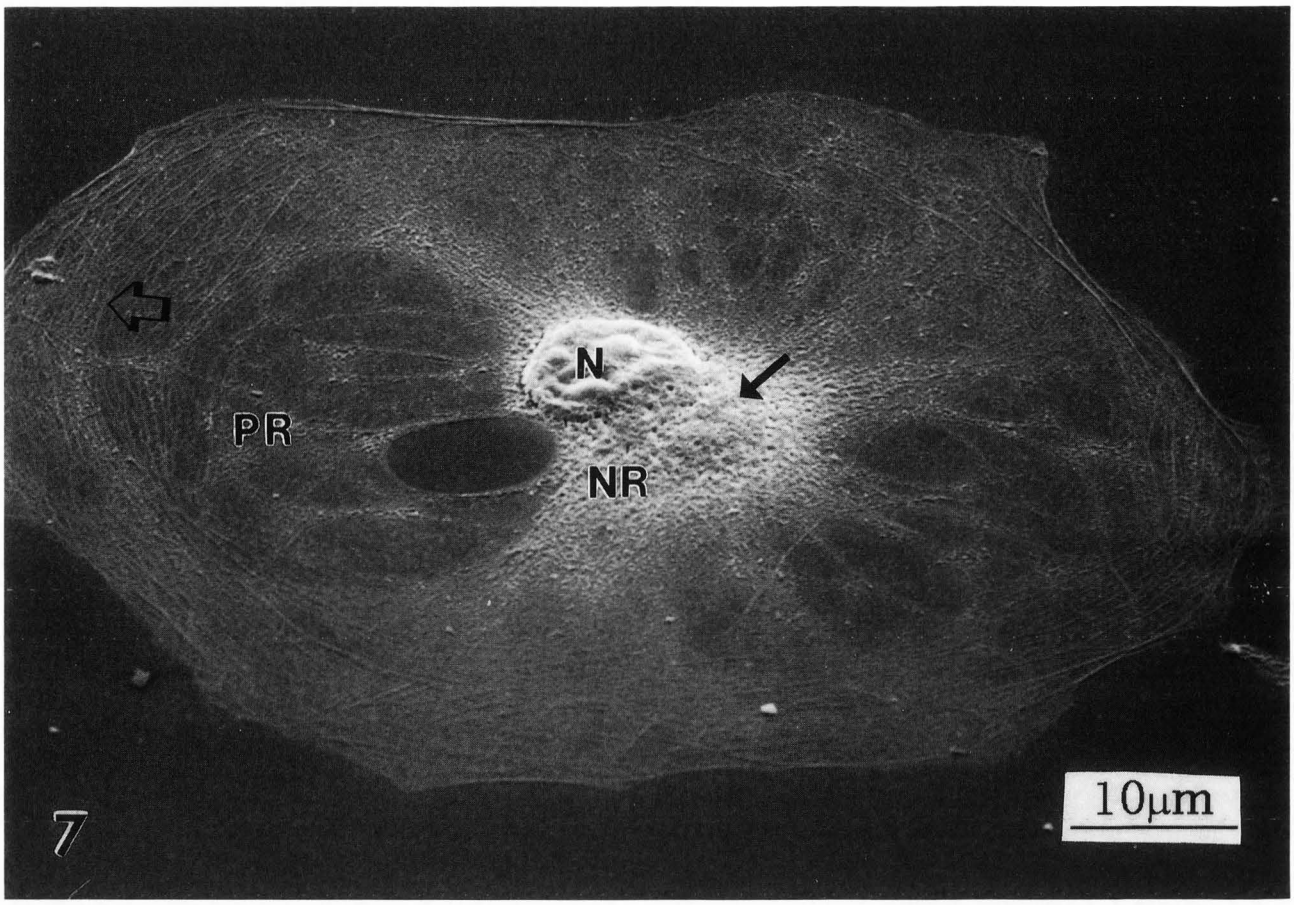

Figure 7 (above). Electron micrograph of a cytoskeletal preparation of a control astrocyte. Note the dense actin core (arrow) next to the nucleus (N) and cytoskeletal elements radiating from this area. Marginal banding can be seen at the periphery of the cell (open arrow). Perinuclear region (NR); Peripheral region (PR).

Figure 8. Electron micrograph of a control astrocyte showing the parallel arrangement of cytoskeletal elements at the periphery of the cell. Note the cross-bridges between the filamentous structures (arrows).

Figure 9. Electron micrograph of a control astrocyte showing an intricate network of interlacing weave-like cytoskeletal structures close to the perinuclear region.

Figure 10. Phase contrast micrograph of an astrocyte 4 hours after treatment with 35 μ/ml of media of DDC. Note granular and vacuolar nature of the perinuclear area (arrow) and the small distorted processes radiating from the cell (arrow head).

Figure 11. Light micrograph of DDC-treated cells (35 μg/ml) 4 hours after treatment stained immunohistochemically for β-tubulin. Notice that the cells have decreased staining especially in the juxtanuclear region.

Figure 12. Light micrograph of DDC-treated cells (35 μg/ml) 4 hours after treatment stained immunohistochemically for GFAP. Note that the filament are disrupted and appear as granulated material.

Figure 13. Whole mount electron micrograph of an astrocyte 4 hours after treatment with 35 μg/ml of media of DDC. Note the raised nuclear region (N) and the irregularly contoured cytoplasmic regions.

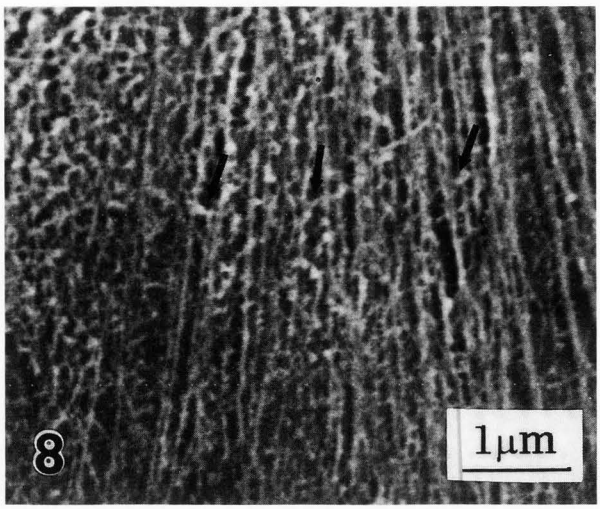
8
1μm

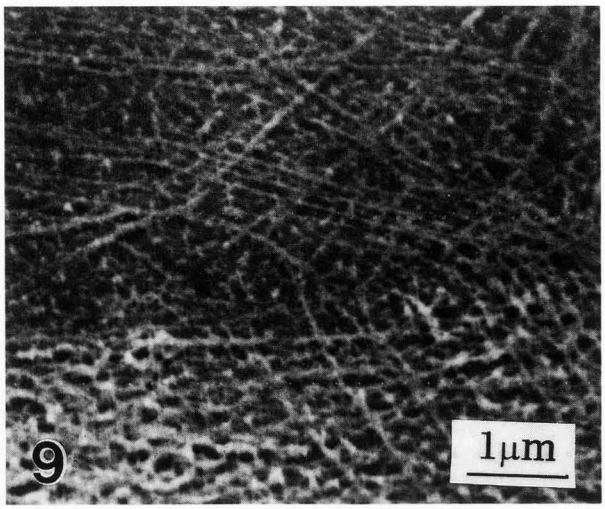
9
1μm

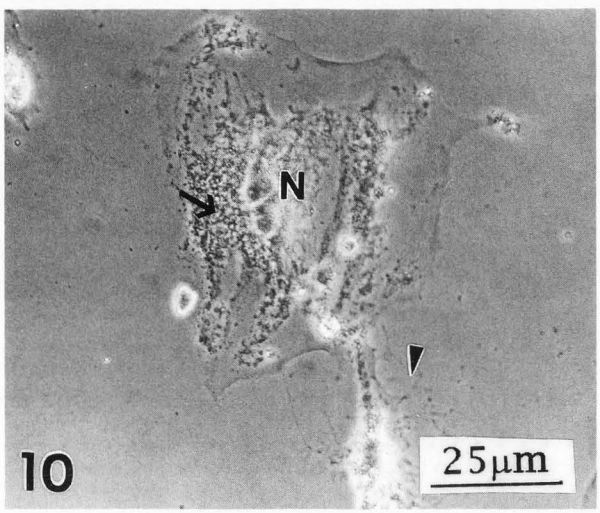
N
10
25μm

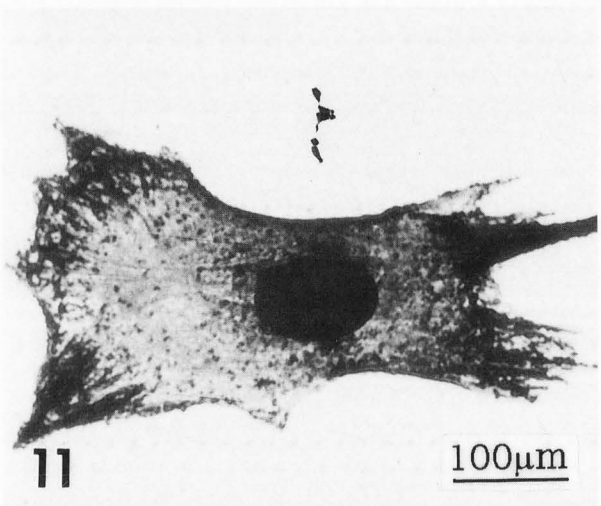
11
100μm

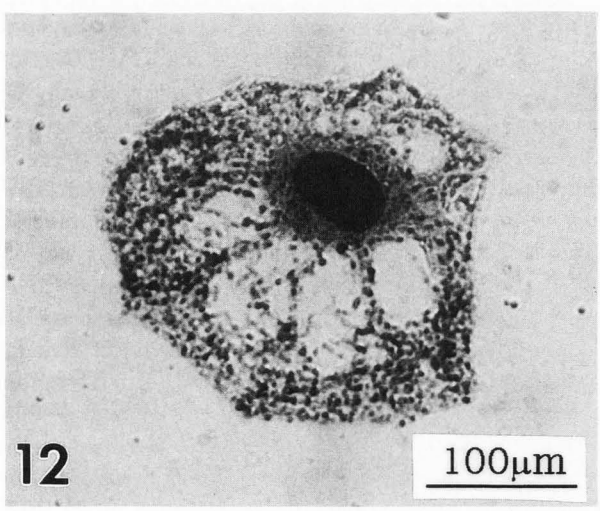
12
100μm

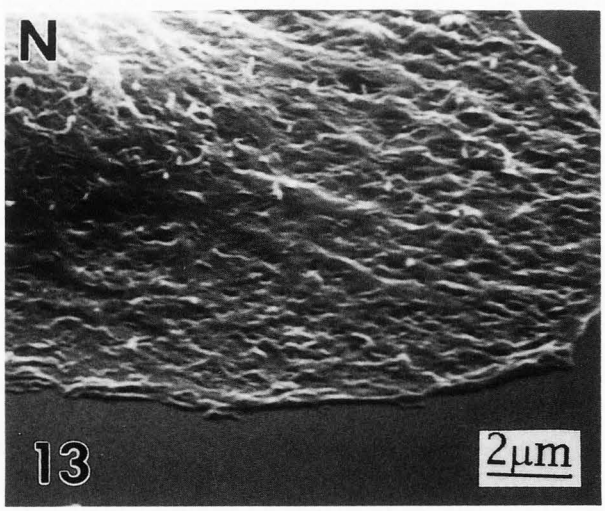
N
13
2μm

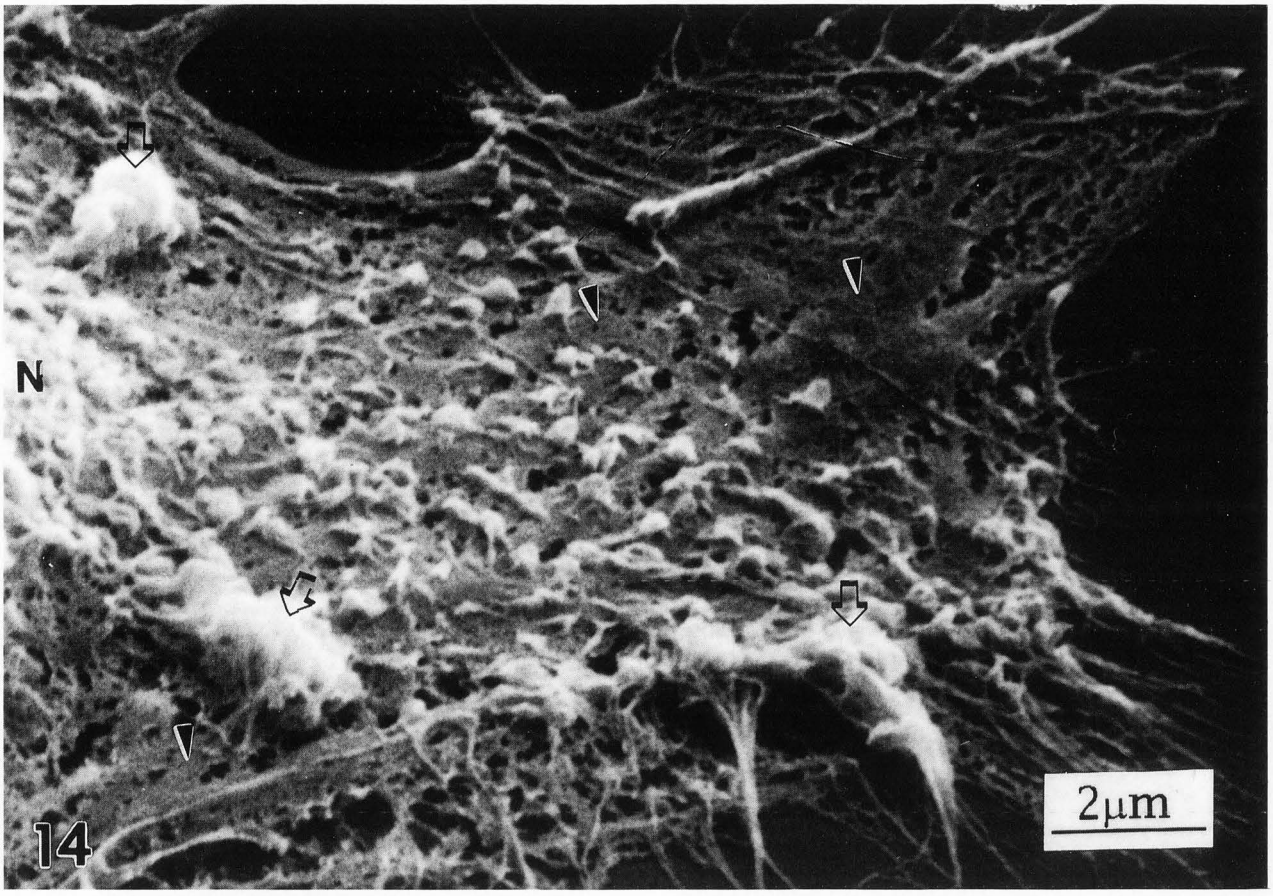

Figure 14. Electron micrograph of a cytoskeletal preparation of an astrocyte 4 hours after treatment with 35 μg/ml of media of DDC. Notice the presence of condensation products (open arrows) and the raised nucleus (N). Note that the actin sheets (arrow heads) are still present.

Results

Rat hippocampal astrocytes grown *in vitro* are pleiomorphic appearing fusiform, stellate, round or oval (Fig. 1). These cells appeared to be composed of two regions (Figs. 1 and 2) regardless of cell shape; the central perinuclear region (NR) encompassing the nucleus and a thin almost translucent, lacy peripheral region (PR). By light microscopy, this peripheral region may be erroneously interpreted to be matrix and not cellular in nature.

Immunolabelling of tubulin with gold showed microtubules radiating like spokes from a wheel from the central nuclear region to the cell periphery (Fig. 3). The density of microtubules decreased as they migrated away from the central region. Microtubules that extended to the edge of the cell often turned and ran parallel to the cell perimeter, resembling a marginal band (Fig. 4).

Immunolabelling of glial fibrillary acidic protein (GFAP) with gold showed a somewhat similar arrangement of the filaments as the tubules (Fig. 5). One exception is that as they extend toward the periphery of the cell, the GFAP containing filaments formed an intertwining network (Fig. 6).

Scanning electron microscopy of whole mount preparations showed a similar morphological arrangement to what was seen by light microscopy. The cell was divided into a central endoplasmic region containing the nucleus (NR) and a much flatter and thinner peripheral exoplasmic region (PR) (Fig. 2). The nuclear region displayed an irregular contour covering a flattened or slightly raised nucleus. The surface of the perinuclear area appeared irregular, containing many pits and depressions (Fig. 2). These pits do not appear to be artifactual since no disruptions in the cell membrane are seen. Fusiformed shaped cells appeared to have the largest nuclear to cytoplasmic ratio. Peripheral regions appeared smoother, and much thinner. Elongated, thin, raised structures were seen under the plasmalemma and represent underlying cytoskeletal components (Fig. 2). Cytoskeletal preparations of control cells at all times appeared similar (Fig 7).

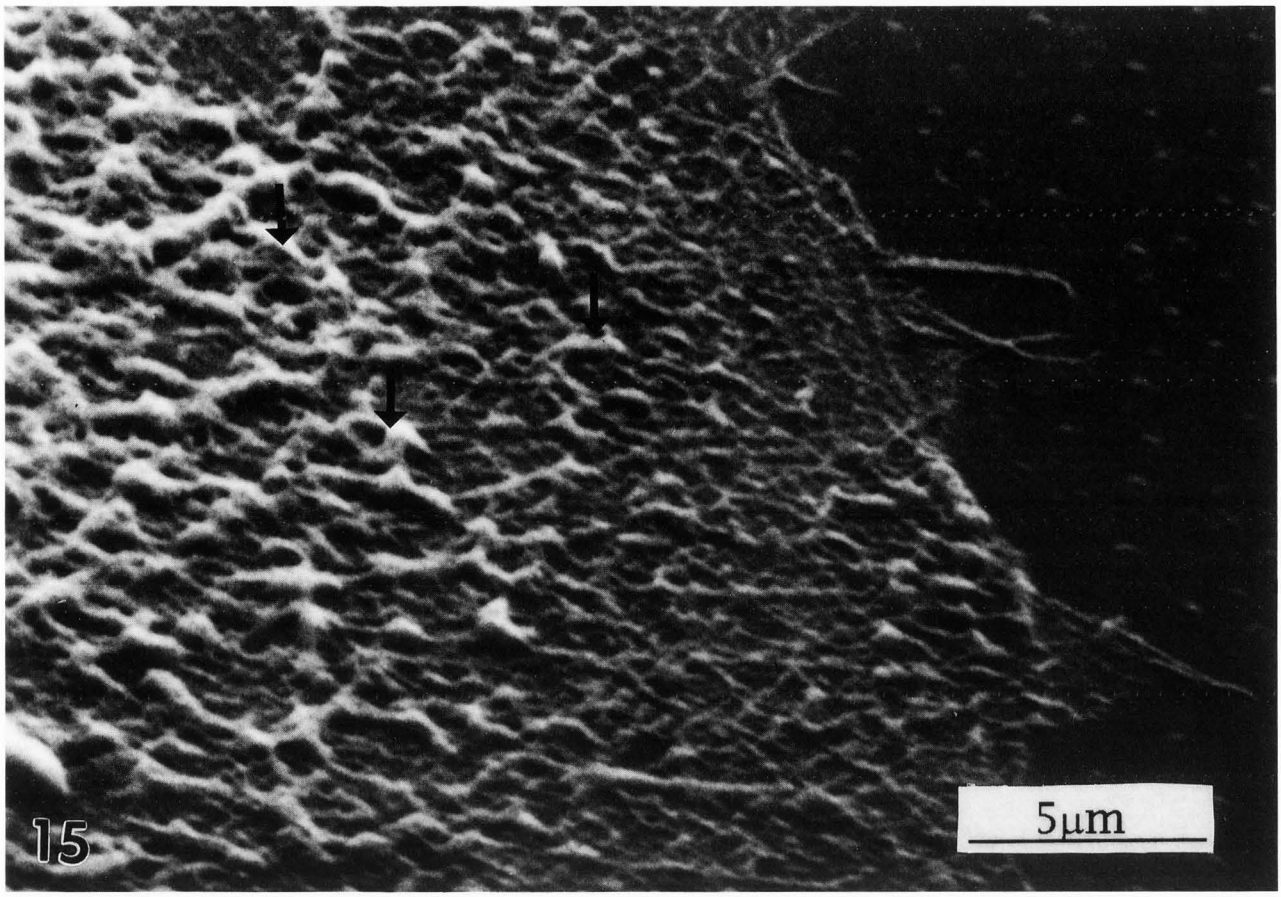

Figure 15. Electron micrograph of a cytoskeletal preparation of an astrocyte 8 hours after treatment with 35 μg/ml of media of DDC. Note that these cells show little or no filamentous structures and numerous condensations products (arrows).

Cytoskeletal preparations of astrocytes revealed a complex network of interlacing fibers and sheets of structural elements. These structures appeared as bundles and sometimes as thinner 25 nm and 40 nm fibers. Since the thickness of deposited gold was 15 nm, the 25 nm and 40 nm fibers may represent intermediate filaments and microtubules. The cortices of these cells, particularly in the perinuclear region, were composed of a dense mat of microfilaments (actin). Individual microfilaments were not resolved because of their size (5 nm) and dense packing. Higher magnification showed these actin sheets overlying larger filamentous structures. In the peripheral region, the actin sheets were almost absent and the larger filamentous structures were easily seen. A highly intricate cytoskeleton, appearing as a weave-like pattern, was observed (Figs. 8 and 9). Bundles of fibers were seen radiating from the central portion of the cell and eventually projecting as a web-like marginal band at its extreme periphery (Fig. 7). Cross bridges were seen connecting these fibers.

DDC treatment (35 μg/ml) showed, by 4 hours, the presence of small granules and vacuoles in the perinuclear region (Fig. 10). A progressive disruption of the microtubules was seen. Immunohistochemical staining with β-tubulin showed fragmented, small particulate immuno-stained material (Fig. 11). Degeneration progressed rapidly (from 4 to 24 hours), eventually leading to a total loss of cytoskeletal elements. Large regions of the cell either did not stain at all (particularly in the perinuclear region) or microtubular material appeared as a condensed reaction product (Fig. 11). GFAP was also altered by DDC treatment. Alterations often appeared as disruption of these filaments into aggregates of reaction product (Fig. 12).

Scanning electron micrographs of whole mount preparations of astrocytes, after 4 and 8 hours post-DDC treatment, showed a highly irregular cell surface and an elevated nucleus (Fig. 13). No cytoskeletal elements were seen after the 12 hours time period. Scanning electron microscopy at 24 hours, showed cells similar to

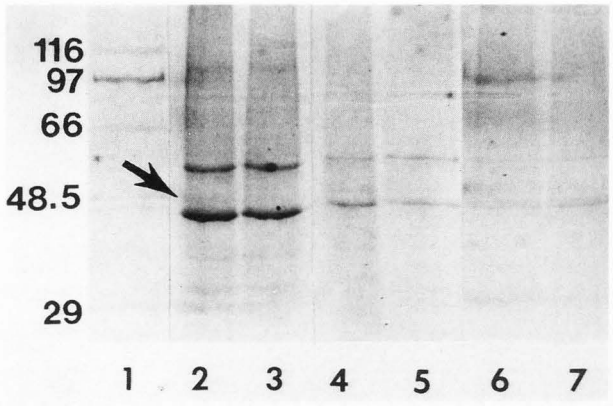

Figure 16. SDS-PAGE electrophoresis of cytoskeletal preparations at 4, 8 and 12 hours post treatment with 35 μg/ml of media of DDC. **Lane 1**: standards (kD); **Lane 2**: control at 4 hours; **Lane 3**: DDC treatment at 4 hours; **Lane 4**: control at 8 hours; **Lane 5**: DDC-treatment at 8 hours; **Lane 6**: control at 12 hours; and Lane 7: DDC at 12 hours. Arrow indicates GFAP region.

---

what was seen at 12 hours except that there was a complete loss of peripheral cytoplasm. Cytoskeletal preparations at 4 hours showed numerous condensation products dispersed through out the cell. They were also seen covering the nucleus. These condensation products appeared irregular in shape and of various sizes. Actin sheets were visible but discrete filamentous structures were absent (Fig. 14).

By 8 hours, cytoskeletal preparations showed that both the central and peripheral regions were severely disrupted. Condensation products and clumping of cytoskeletal elements were observed throughout the cell. Actin filaments had irregular contours and the cell periphery was completely disorganized. Filamentous structures were rarely observed (Fig. 15).

Electrophoresis

The electrophoretic pattern of the treatment groups at 4, 8, and 12 hours after DDC treatment revealed a decreased staining in the 50 kD range (Fig. 16). This is approximately the range for the GFAP intermediate filament protein. Because only living adherent cells were studied, very small amounts of protein were obtained from the treatment groups in the latter time periods. All wells were adjusted at each time period with the same quantity of cytoskeletal protein. Western blots at 4, 8 12 and 24 hours all appeared similar. Localization of tubulin revealed a blotchy appearance of the tubulin band in the treated cells verses the control astrocytes. The blotchy material appeared heavier in weight and dragged behind the main tubulin band. GFAP was reduced in the treated cells. Actin, on the other hand, was heavily

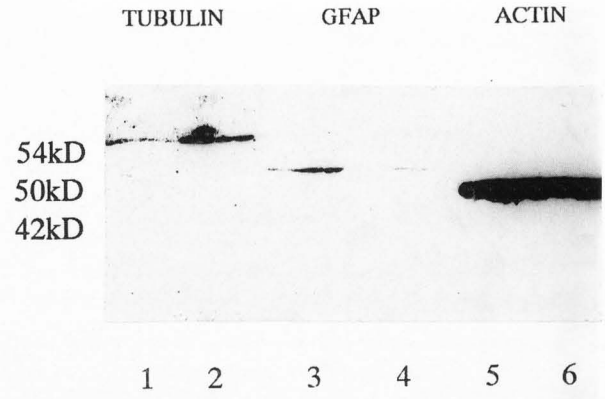

Figure 17. Western blots of representative cytoskeletal proteins post treatment with 35 μg/ml of media of DDC. **Lanes 1 and 2** represent immunoblots directed against β-tubulin. Lane 1 is control protein and lane 2 is protein from treated cells. **Lanes 3 and 4** are immunoblots directed against GFAP. Lane 3 is control and lane 4 is treated. **Lanes 5 and 6** are immunoblots directed against actin. Lane 5 is control and lane 6 is treated. The numbers at the left are molecular wights in kD. Note the aberrant tubulin band in the treated group and the decreased in GFAP in the treated group. The actin bands appear similar in both control and treated groups. These results were similar for all time periods.

---

stained in all cell types whether found in treated or control cells (Fig. 17).

Discussion

This is the first time DDC-induced cytoskeletal alterations have been documented in the astroglial cell culture system. Previous studies have all utilized either animal, cell free *in vitro* systems or tissue culture techniques using other cell types. None of these investigations used time course studies specifically targeting the cytoskeleton or examined the cytoskeleton using SEM.

Recent evidence suggests that the astrocyte is frequently the initial target for toxic insult in the CNS. Any alterations in astrocytic function will ultimately lead to neuronal injury due to the close functional relationship between these cell types (Aschner and Kimelberg, 1991; Koestner and Norton, 1991). DDC-induced neuronal degeneration, therefore, may be due to both direct cytotoxic effects and indirect effects secondary to astroglial insult.

Some of the dithiocarbamates have been reported to produce neuropathologic changes in the hippocampus. Trombetta and Adachi (1985) noted abnormal intracellular tubular material in the hippocampus after 18 months of treatment with the drug disulfiram (an oxidized parent

compound which is metabolically interconvertible with DDC) (Simonian *et al.*, 1992).

The pathogenesis of many neurotoxic substances is often associated with profound disorganization of cytoskeletal structures with loss or accumulation of the individual elements. Intermediate filaments are of special interest because of their tendency to form dense aggregates in several experimental and human toxic neuropathies (Bilbao *et al.*, 1984). Dithiocarbamates have been shown to cause toxic injury to neurons with effects seen in the perikaryon and the axon resulting in abnormal accumulation of microtubules, loss and/or accumulation of neurofilaments, and cytoplasmic lipid debris (Trombetta and Adachi, 1985). DDC-induced alterations of filamentous proteins have been documented in several other *in vivo* studies (Kim and Rizzuto, 1975; Ueno *et al.*, 1977; Ansbacher *et al.*, 1982, Bilbao, 1984; Lehto *et al.*, 1984). In the present study, similar alterations of the intermediate filaments and microtubules of the astrocyte have been found. A progressive loss of organized cellular architecture associated with loss of intermediate filaments and altered microtubular structures was seen.

Chronic dithiocarbamate administration has been shown to produce a distal neurofilamentous axonopathy (Ansbacher *et al.*, 1982). The axonal swellings consisted of masses of neurofilaments and various distorted membranous organelles. Bilbao *et al.* (1984) also examined a filamentous axonopathy induced by disulfiram which displayed axonal enlargements due to the accumulation of whorled filaments. Dispersed among these filaments were microtubules and mitochondria.

Potchoo *et al.* (1986) studied the dose-dependent inhibition of microtubule formation by disulfiram in a cell free system. The microtubules showed a drastic decrease in number and length with a decreased rate of polymerization. They suggest that this inhibition is correlated to the direct blockade of sulfhydryl groups in microtubules by disulfiram.

Lehto *et al.* (1984) studied the effects of disulfiram and some other dithiocarbamates on the cytoskeleton of neuronal cells *in vivo* and *in vitro*. Disulfiram caused rounding up of cells and an accumulation of tubulin in discrete clumps often seen as cellular protrusions. By electron microscopy, *in vivo* findings included a slight decrease in the filament density and a clear decrease in the number of microtubules (1 and 3 week studies). The dithiocarbamate fungicides ferbam and thiram (which are metabolized to DDC) had a pronounced effect on the morphology and structure of both microtubules and intermediate filaments. The authors suggested further studies into whether metal complexes with some dithiocarbamates contribute to the adverse effects on the cytoskeleton.

The hippocampus is also known to accumulate metals, thereby acting as a primary metal sink in the CNS (Danscher *et al.*, 1976). Histochemical findings indicate that the excessive uptake of copper results in accumulation in both the glial cells and pyramidal cells (Szerdahelyi and Kása, 1987). Lakomaa *et al.* (1982) examined several brain regions of DDC-treated rats. Chronic dosing over a four week period resulted in elevated copper concentrations, particularly with respect to the hippocampal region (44.2%) and the brain stem (55.2%). Overall, the data demonstrated a significant degree of tissue selectivity for copper disposition. This may be related to its aggregation in specific cell types. Therefore, it is reasonable to examine the hippocampal astrocyte due to the well-documented effects of DDC and copper *in vivo* within this region.

O'Shea and Kaufman (1980) examined the effects of copper on microtubular degeneration in neuroepithelial cells. Ultrastructurally, these cells showed a reduction in the number of microtubules and/or an increase in microtubular remnants. Often, the microtubules appeared to have a fuzzy, rather than a sharply-defined, outline and occasionally gaps were present along their length. Some of the toxic effects of DDC may be due to the preferential redistribution of metals to the CNS by the highly lipophilic DDC metal (copper) complex (Miller, 1982; Andersen and Nielsen, 1989).

Microtubule assembly and disassembly is dependent on the concentrations of divalent cations present (Weisenberg, 1972). Metal-induced inclusions may represent the breakdown products of microtubules themselves (Gaskin and Shelanski, 1976). O'Shea and Kaufman (1980) suggest that an elevation in the intracellular concentration of microtubular precursor elements, following microtubular depolymerization, may lead to their precipitation and consequent appearance in this aggregated form. Therefore, protein synthesis does not appear to be crucial for this aggregation to take place (O'Shea and Kaufman, 1980).

In this study, SEM data demonstrates that microtubular and intermediate filament structure is altered after DDC exposure. The DDC-treated cells showed accumulation of condensation products with extensive disruption of the cytoskeletal architecture over time. SEM also shows loss of filaments and fused cytoskeletal condensate. The actin cortex appeared fairly unscathed except during the later stages of DDC insult.

Western blots showed changes in the mobility of the β-tubulin protein and a decrease in GFAP in the DDC-treated cells at all time periods. Little or no alterations of actin were seen. These results suggest that DDC may selectively alter microtubules and intermediate filaments.

The toxic effects of DDC are multietiological with a complex pathogenesis and multiple aberrant mani-

festations. These findings must be taken into account when researching the role of the dithiocarbamates in any clinical or environmental application.

References

Adachi M, Solitaire GB (1979) Histologic and ultrastructural studies of long term effects of disulfiram on the CNS and skeletal muscles of rats. J. Neuropathol. Exper. Neurol. **38**: 301 (abstract).

Alberts B, Bray D, Lewis J, Raff M, Roberts K, Watson JD (1989) The cytoskeleton. Chapter 11. In: Molecular Biology of the Cell. Garland Publ., New York. pp. 613-661.

Allain P, Krari N (1991) Diethyldithiocarbamate, copper and neurological disorders. Life Sci. **48**: 291-299.

Andersen O, Nielsen JB (1989) Effects of diethyldithiocarbamate on the toxicokinetics of cadmium chloride in mice. Toxicology **55**: 1-14.

Andersen O, Nielsen JB, Svendsen P (1988) Oral cadmium chloride intoxication in mice: diethyldithiocarbamate enhances rather than alleviates acute toxicity. Toxicology **52**: 331-342.

Ansbacher LE, Bosch EP, Cancilla PA (1982) Disulfiram neuropathy: A neurofilamentous distal axonopathy. Neurology **32**: 424-428.

Anzil AP (1985) Morphological assessment of neurotoxicity: Disulfiram neuropathy as an animal model of human toxic axonopathies. In: Neurotoxicology. Blum, K, Manzo L (eds.). Marcel Dekker, New York. pp. 535-558.

Aschner M, Kimelberg HK (1991) The use of astrocytes in culture as model systems for evaluating neurotoxic-induced injury. Neurotoxicology **12**: 505-518.

Bell PB (1981) The application of scanning electron microscopy to the study of the cytoskeleton of cells in culture. Scanning Electron Microsc. **1981**; II: 139-157.

Bell PB, Lindroth M, Fredriksson BA (1988) Preparation of cytoskeletons of cells in culture for high resolution scanning and scanning transmission electron microscopy. Scanning Microsc. **2**: 1647-1661.

Bernal AD, Stahel RA (1985) Cytoskeleton associated proteins: their role as cellular integrators in the neoplastic process. Crit. Rev. Oncol. Hematol. **3**: 191-204.

Bilbao JM, Briggs SJ, Gray TA (1984) Filamentous axonopathy in disulfiram neuropathy. Utrastruct. Path. **7**: 295-300.

Borch RF, Pleasants ME (1979) Inhibition of cisplatinum nephrotoxicity by diethyldithiocarbamate rescue in a rat model. Proc. Natl. Acad. Sci. **76**: 6611-6614.

Cohen JD, Robins HI (1990) Cytotoxicity of diethyldithiocarbamate in human and rodent cell lines. Invest. New Drug **8**: 137-142.

Danscher G, Fjerdingstad EJ, Fjerdingstad E, Fredens K (1976) Heavy metal content in subdivisions of the rat hippocampus (zinc, lead and copper). Brain Res. **112**: 442-446.

Gaskin F, Shelanski ML (1976) Microtubules and intermediate filaments. In: Essays in Biochemistry. Campbell PN, Aldridge WN (eds.). Churchill, London. pp. 185-207.

Ghetti B (1979) Induction of neurofibrillary degeneration following treatment with maytansine *in vivo*. Brain Res. **163**: 9-19.

Goldman JE, Yen S (1986) Cytoskeletal protein abnormalities in neurodegenerative diseases. Ann Neurol. **19**: 209-223.

Griffin JW, Price DL, Hoffman PN (1983) Neurotoxic probes of the axonal cytoskeleton. Trends Neurosci. (TINS) **6**: 490-495

Hansson E, Rönnbäck L, Persson LI, Lowenthal A, Noppe M, Alling C, Karlsson B (1984) Cellular composition of primary cultures from cerebral cortex, striatum, hippocampus, brain-stem and cerebellum. Brain Res. **300**: 9-18.

Hersh EM, Funk CY, Petersen EA, Tyschon KL Mosier DE (1993) Dose response and timing effects in the therapy of the LP-BM5 murine retrovirus-induced lymphoproliferative immunodeficiency disease with diethyldithiocarbamate. Int. J. Immunopharmacol. **15**: 137-143.

Hochstein P, Kumar KS, Forman SJ (1980) Lipid peroxidation and the cytotoxicity of copper. Ann. N.Y. Acad. Sci. **335**: 240-248.

Hutchinson DW (1985) Metal chelators as potential antiviral agents. Antiviral Res. **5**: 193-205.

Johansson B, Stankiewicz Z (1985) Bis (diethyldithiocarbamate) copper complex: A new metabolite of disulfiram? Biochem. Pharmacol. **34**: 2989-2991.

Kim SU, Rizzuto N (1975) Neuroaxonal degeneration induced by sodium diethyldithiocarbamate in cultures of central nervous tissue. J. Neuropath. Exp. Neurol. **34**: 531-541.

Koestner A, Norton S (1991) Nervous System. In: Handbook of Toxicologic Pathology. Academic Press, New York. pp. 625-674.

Lakomaa EL, Sato S, Goldberg AM, Frazier JM (1982) The effect of sodium diethyldithiocarbamate treatment on copper and zinc concentrations in rat brain. Toxicol. Appl. Pharmacol. **65**: 286-290.

Laemmli EK (1970) Cleavage of structural proteins during the assembly of the head of bacteriophage T4. Nature **227**: 680-685.

Lehto V, Virtanen I, Savolainen K (1984) The effect of some dithiocarbamates, disulfiram and 2,5-hexanedione on the cytoskeleton of neuronal cells *in vivo* and

in vitro. In: The Cytoskeleton, A Target for Toxic Agents. Clarkson TW, Sager PR, Syversen TLM (eds.). Plenum Press, New York. pp. 143-158.

Li W, Chou IN (1992) Effects of sodium arsenite on the cytoskeleton and cellular glutathione levels in cultured cells. Toxicol. Appl. Pharmacol. **114**: 132-139.

Li W, Zhao Y, Chou IN (1987) Paraquat-induced cytoskeletal injury in cultured cells. Toxicol. Appl. Pharmacol. **91**: 96-106.

Marcum JM, Dedman JR, Brinkley BR, Means AR (1978) Control of microtubule assembly-disassembly by calcium-dependent regulator protein. Proc. Natl. Acad. Sci. U.S.A. **75**: 3771-3775.

Miller DB (1982) Neurotoxicity of the pesticidal carbamates. Neurobehav. Toxicol. Teratol. **4**: 779-787.

O'Shea KS, Kaufman MH (1980) Copper-induced microtubule degeneration and filamentous inclusions in the neuroepithelium of the mouse embryo. Acta Neuropathol. **49**: 237-240.

Potchoo Y, Braguer D, Peyrot V, Chauvet-Monges AM, Sari JC, Crevat A (1986) *In vitro* inhibition of microtubule assembly by disulfiram. Intl. J. Clin. Pharmacol. Ther. Toxicol. **24**: 499-504.

Simonian J, Haldar D, Delmaestro E, Trombetta LD (1992) Effect of disulfiram on mitochondria from rat hippocampus: metabolic compartmentation of DS neurotoxicity. Neurochem. Res. **17**: 1029-1035.

Stein MR, Trombetta LD (1993) Effects of diethyldithiocarbamate on calmodulin in neuroblastoma cells. J. Toxic. Environ. Health **39**: 465-481.

Stromme JH (1963) Effects of diethyldithiocarbamate and disulfiram on glucose metabolism and glutathione content of human erythrocytes. Biochem. Pharmacol. **12**: 705-715.

Szerdahelyi P, Kása P (1987) Regional differences in the uptake of exogenous copper into rat brain after acute treatment with sodium diethyldithiocarbamate. Histochemistry **86**: 627-32.

Tempel K, Schmerold, I Goette A (1985) The cytotoxic action of diethyldithiocarbamate *in vitro*. Arzneim-Forsch. **35**: 1052-1054.

Trombetta LD, Toulon M, Jamall IS (1988) Protective effects of glutathione on diethyldithiocarbamate (DDC) cytotoxicity: A possible mechanism. Toxicol. Appl. Pharmacol. **93**: 154-164.

Trombetta LD, Adachi M (1985) Severe degeneration of axons other alterations induced by disulfiram in the central nervous system of rats. In: Current Trends in Neurosciences: The Pathology of the Myelinated Axon. Adachi M, Hirano A, Axonson SM (eds.). Igaku-Shoin, New York. pp. 367-381.

Ueno T, Nhyagishi T, Takahata N, Fujieda T (1977) Electron microscopic studies on the cerebral lesions of rats in experimental chronic disulfiram poisoning. Acta Neuropat. (Berhn) **38**: 221-224.

Weisenberg R (1972) Microtubule formation *in vitro* in solutions containing low calcium concentrations. Science **177**: 1104-1105.

Weiss B, Corey-Slechta DA, Cox C (1990) Modification of lead redistribution by diethyldithiocarbamate. Fundam. Appl. Toxicol. **15**: 791-799.

Discussion with Reviewers

M. Lindroth: How was the concentration of 35 μM DDC chosen?

Authors: The concentration of 35μM DDC was chosen from previous studies on the toxicity of DDC on astrocytes in culture and resulting viability curves (Trombetta *et al.*, 1988). Viability was determined using trypan blue exclusion. This dose approximates the LD 50.

F. Barile: It has been suggested that the toxicity of DDC may be mediated in part by the formation of superoxide radicals through cupric ion interaction with membrane sulfhydryl groups. Could this represent a universal phenomenon resulting in lipid peroxidation, such as that seen in paraquat toxicity?

Authors: DDC causes lipid peroxidation directly related to copper concentration (Delmaestro and Trombetta, 1995). In addition, cytoskeletal architecture is dependent on its sulfhydryl status. Any interruption of this status can result in its depolymerization (Trombetta and Kromidas, 1992).

F. Barile: How does the changes in the electrophoretic patterns of tubulin and GFAP observed between control and DDC treatment explain the morphological differences seen in the micrographs?

Authors: Although electrophoretic patterns can give some indication of altered mobility and differences in protein concentration, they do not clearly indicate what these changes represent in terms of cytoskeletal architecture. Tubulin and intermediate protein may be present but not arranged in the proper pattern or architecture. The condensation products seen in cytoskeletal preparations of treated astrocytes are cytoskeletal proteins but the SEM shows obvious alterations to cellular architecture.

M. Malecki: Considering your results and those from the work by Dr. Nedergaard (Science **263**: 1768; 1994), can you comment on the effects of DDC on astrocyte/neuron interactions *in vivo*?

Authors: There is no doubt that astrocyte/neuron interactions have to be studied more closely. Previous work in our laboratory (Trombetta and Adachi, 1985) indicated that, in an *in vivo* study, the rat astrocyte was

altered by the administration of disulfiram (the parent compound of DDC) prior to any change seen in neurons. Nadergaard and others have shown an intimate physiological relationship between these two cell types. This interdependence may extend beyond normal function and may also involve relationships resulting from toxic insult to one cell type or the other.